NASA Technical Memorandum 103788

Growth Kinetics of Physical Vapor Transport Processes: Crystal Growth of the Optoelectronic Material Mercurous Chloride

N.B. Singh
Westinghouse Science and Technology Center
Pittsburgh, Pennsylvania

and

W.M.B. Duval
Lewis Research Center
Cleveland, Ohio

March 1991

NASA

CONTENTS

1. EXECUTIVE SUMMARY

The results reported here were carried out in order to derive a quantitative understanding of the physical vapor transport (PVT) process for the purpose of identifying the magnitude of convective effects on the crystal growth process. The effects of convection on crystal quality were studied by varying the aspect ratio and those thermal conditions which ultimately affect thermal convection during PVT. An important outcome of the present study was the observation that the convection growth rate increased up to a certain value and then dropped to a constant value for high aspect ratios. This indicated that a very complex transport had occurred which could not be explained by linear stability theory. Better quality crystals grown at a low Rayleigh number confirmed that improved properties are possible in convectionless environments.

2. TECHNICAL BACKGROUND

2.1 THE MERCUROUS HALIDES

The mercurous halides have recently become important because of their application in acousto-optic and opto-electronic devices. The properties that make this class of materials important are: (a) the spectral transmission range, (b) the photo-elastic coefficient, (c) the acousto-optic figure of merit, (d) acoustic velocity, and (e) acoustic attenuation. These halides belong to the tetragonal (D4h) crystal class and are positively uniaxial with large birefringence. The refractive indices for Hg_2Cl_2 are 2.621 and 1.962; for Hg_2Br_2, 2.975 and 2.121. The transmission ranges are 0.36 to 20 μm for Hg_2Cl_2, 0.4 to 30 μm for Hg_2Br_2, and 0.5 to 40 μm for Hg_2I_2. This wide optical transmission range is very unusual and potentially very useful for wideband spectroscopic devices.

During the last several years we have been involved[1-4] in the purification, crystal growth, and characterization of mercurous halides. The need for high optical-quality crystals came from military defense applications of the devices for which mercurous halides appear to have great potential. Mercurous iodide is the least developed and requires a great number of refinements. We have grown reasonably good-quality mercurous chloride and mercurous bromide, but scattering levels due to inhomogeneity in the refractive index are still a big problem. These halides have the slowest shear acoustic velocity in the [110] direction of any known acousto-optic material. The magnitudes of acoustic velocity are 254 m/s for Hg_2I_2, 273 m/s for Hg_2Br_2, and 347 m/s for Hg_2Cl_2. By comparison, this value for commercially available TeO_2 is 616 m/s. If we define the quality of the material (figure of merit) as suggested by Chang,[5] these halides have very large values. Also, mercurous halides cover a large transmission range, i.e., 0.36 to 40 μm. The acoustic attenuation for Hg_2Cl_2 and Hg_2Br_2 is 376 and 431.5 dB cm^{-7} GHz^{-2}. These properties are all well suitable for fabrication of Bragg cells which can offer high resolution, high diffraction efficiency, and high dynamic

range. From this perspective we propose to study the factors which ultimately affect the homogeneity of the crystals during growth.

2.2 PHYSICAL VAPOR TRANSPORT PROCESS

Mercurous halides decompose[6-7] to mercury and mercuric halide ($Hg_2X_2 \rightarrow Hg + HgX_2$) at the melting point. The existence of the two liquid fields and compositional stratification largely preclude the solidification of large Hg_2X_2 crystals by conventional melt growth techniques. However, mercurous halides exhibit reasonably high vapor pressure at low temperature, and crystal growth by vapor transport could be accomplished at rates well within practical range. The purification process of the source material and the furnace design are very difficult tasks. Since mercurous halides are not soluble in most of the usual solvents, including alcohols, acetone, acids, and water, purification by a recrystallization method is very difficult. Purification by directional freezing or zone-refining methods is also not applicable because of decomposition into mercury and mercuric salt. A sublimation method has therefore been used for purifying these halides.

Our previous studies[2] have shown that mercurous chloride has a very high magnitude of anisotropy with respect to growth rates. The growth velocity in the [110] direction is approximately half that in the [001] direction. This suggests that comparison of growth velocities in different thermal environments or geometries should be done for a particular crystal orientation. The results reported here are for the growth of mercurous chloride in the [110] orientation.

2.3 IMPORTANCE OF CONVECTION IN CRYSTAL GROWTH OF MERCUROUS CHLORIDE

The main objective is to clearly identify the growth conditions under which crystals with uniform refractive index can be grown. The influence of convection is very complex; it produces a variety of spatial and temporal transport rate patterns which cause undesirable micro- and macrosegration. In the case of high-purity source material, the major concern is thermal convection, which can promote stirring in fluids and contribute significantly to compositional differences in the growing crystal through transient behavior. Some fluids develop

periodic temperature fluctuations at relatively low temperature gradients, leading to the production of undesirable growth rate fluctuations and changes in boundary layer thickness. The situation becomes even more complex in the presence of impurities, and double diffusive convection (thermo-solutal convection) controls the fluid flow. The magnitude of convection can be expressed in terms of a Rayleigh number.

For the geometry used in our system, one can define the Rayleigh number, Ra as[9]:

$$Ra = \frac{g \cdot \beta \cdot a^4 \cdot Cp \cdot d^2 \Delta T}{k \cdot \eta \cdot L} \qquad (1)$$

where g is the gravitational constant, β is the volume expansion coefficient, ΔT is the temperature difference between hot and cold zones, a is the radius of the ampoule, Cp is the heat capacity, d is the density, k is the thermal conductivity, η is the viscosity, and L is the transport length. Very extensive theoretical studies have been done on this problem, but experiments are very limited for materials of low Prandtl number ($Pr = \eta \cdot Cp/k$). From the equation it is clear that thermal convection conditions (Ra) can be changed by varying g, ΔT, and/or a/L. Also, equation 1 shows that Ra is strongly dependent on geometry (a^4/L) in comparision to ΔT.

3. EXPERIMENTAL METHOD

3.1 MATERIALS AND PURIFICATION

Since the objective of the present program was to study the convection effect in pure mercurous chloride, attempts were made to prepare high-purity mercurous chloride. This minimizes the solutal convective effects.

As-supplied source materials were listed as 99%+ purity. For the purification of source material we designed a multichamber Pyrex sublimation column shown in Figure 1. This apparatus was cleaned by rinsing with acetone, chromic acid, and sulphuric acid followed by a mixture of nitric acid, hydrofluoric acid, and water. The final rinsing was carried out using DI water repeatedly. The source material was loaded in one column of the glass apparatus and evacuated. During evacuation, the side tube was placed in liquid nitrogen to solidify undesired volatile impurities. Occasional heating was also provided to the mercurous chloride charge to drive out moisture. After achieving a good vacuum (in the range of 10^{-6} torr), the column was sealed. The column containing as-supplied material was placed in a temperature gradient furnace to sublime the material. The temperature of the furnace was maintained at approximately 350°C. After transporting most of the as-supplied material into the second column, the first column was sealed and separated. A large amount of dark-colored residue was left in the first column. In a similar fashion, material was transported from the second to third column and so on. After five to six sublimations, the mercurous chloride became water clear and quite suitable for the present purpose. Purity was checked by spark source mass spectrometry.

3.2 FURNACE AND CALIBRATION

Experiments were carried out in a two-zone transparent furnace. The zones were separated by a transparent annular evacuated glass dewar. This insulated section produced a hump in the temperature profile. Each

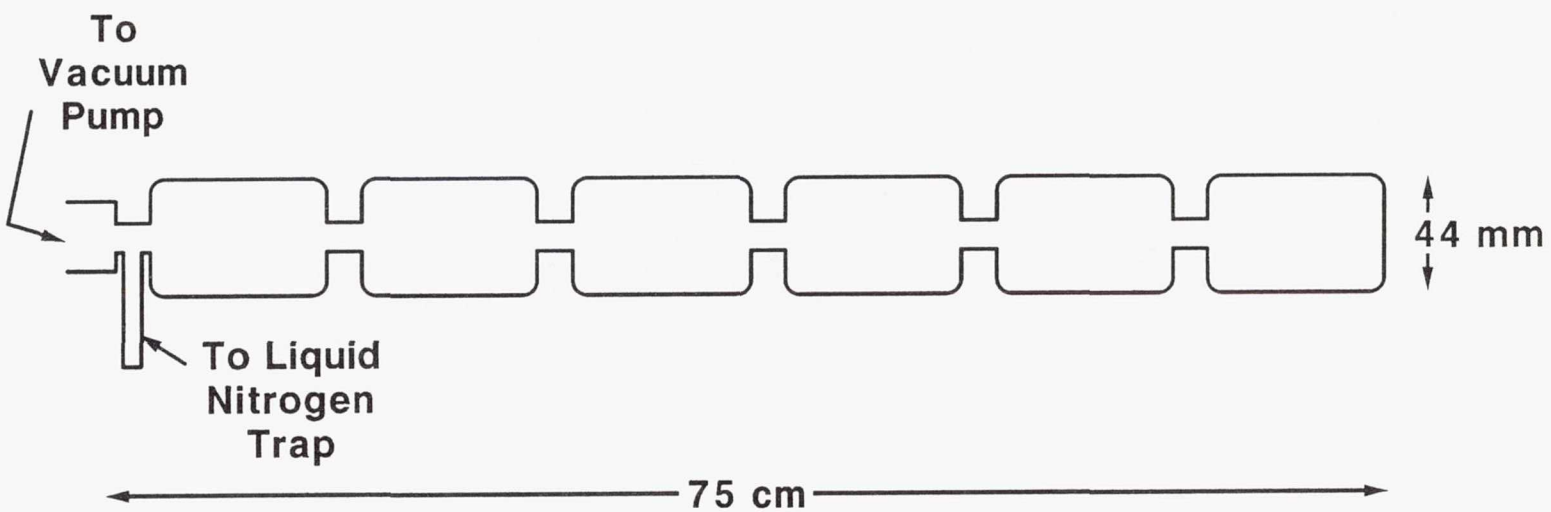

Figure 1. Purification apparatus for Hg_2Cl_2.

furnace was controlled independently by separate controllers. The temperature distribution was measured in two ways: (a) using a bare chromel-alumel thermocouple, and (b) using a platinum probe in a dummy growth tube filled with mercurous chloride and quartz pieces.

For crystal growth runs a platinum probe was always used. The probe was built in a specially designed ampoule, which had a thermometer well in the center of the ampoule. A calibrated platinum probe was placed in the thermometer well (capillary tube), which permitted measurements along the growth axis of the crystal. Since for each set of measurements more than 20 minutes was provided, it was assumed that the thermometer well did not produce any distortion in the temperature field of the crystal.

3.3 GROWTH RATE MEASUREMENTS

All growth rate measurements were carried out for the [110] orientation. We designed the growth tube similar to that shown in Figure 2 for this purpose. A pre-oriented seed was used to seed the crystal in the [110] direction. The source material was sealed in the tapered cylindrical quartz ampoule. For the growth rate measurements, mercurous chloride crystal was grown to a length of 2 cm by pulling the tube, and then pulling was stopped to achieve the equilibrium interface position (stage 1). A time of 12 to 24 hours was allowed to achieve the equilibrium. After recording the equilibrium position, the ampoule was rapidly raised by approximately 3 - 5 mm (stage 2).

The crystal then grew down the tube to establish the new equilibrium position (stage 3). During this period, the crystal length was measured as a function of time. From these measurements growth velocity could be deduced.

3.4 CRYSTAL CHARACTERIZATION

3.4.1 X-ray Characterization

X-ray Laue patterns were taken to ensure that growth rates were measured in the [110] direction. This enabled us to identify the facets on the surface of the crystals during growth.

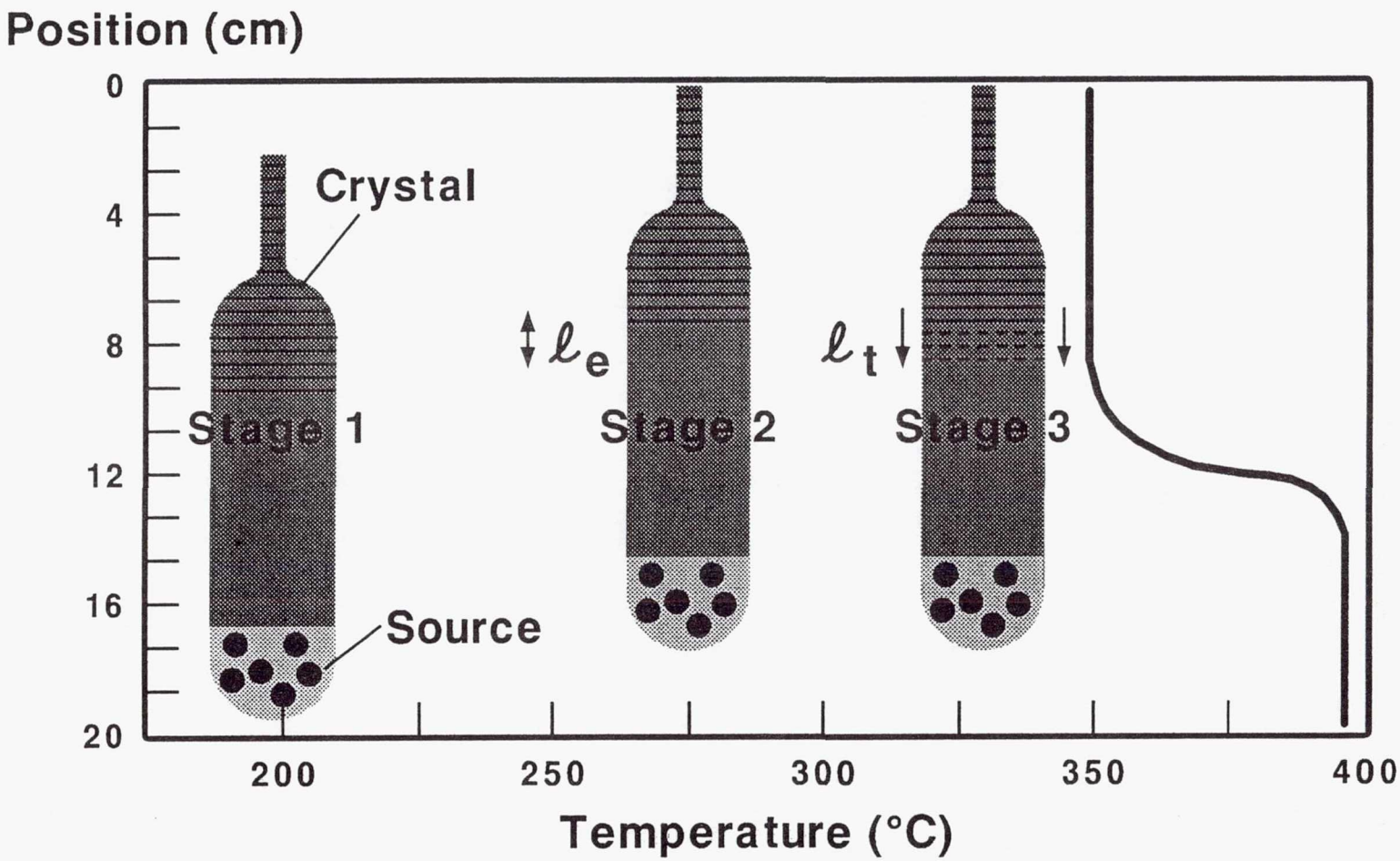

Figure 2. Growth tube for growth rate measurements.

3.4.2 Scattering Measurements

A He-Ne laser beam expanded through a spatial filter (5 mm) was used in order to obtain an average of crystal scattering. The beam was passed through the crystal and the emerging beam was focussed onto the slit of a beam scanner. The scanner has a 25 μm slit with an optical fibre attached behind the slit. The slit/fiber assembly was in turn joined to a motorized linear drive. The fiber transmitted light through the slit onto a photomultiplier, the output of which was fed to a logarithmic dc amplifier. The output of the amplifier was displayed on an X-Y recorder, the x-input being driven with a signal proportional to the linear displacement of the slit. The system is shown in Figure 3.

3.4.3 Birefringence Interferometry

To evaluate crystal homogeneity by birefringence interferometry, a polarized beam from a 1 mW He-Ne laser operating at 1.5 μm was focussed through a pinhole to obtain a good-quality Gaussian mode, and was then expanded and collimated to fill a 5 cm aperture. The mercurous chloride crystal to be inspected was placed in this beam. The polarization of the probe beam was adjusted to be incident on the crystal at 45 degrees to the projection of the optical axis on the plane perpendicular to the direction of the beam. This was accomplished either by rotating the laser to the proper position or by use of a polarizer in front of the crystal. As a result of this choice of polarization, the incoming beam split into two beams as it traversed the birefringent crystal. One of these beams saw the ordinary refractive index, n_o, and travelled with speed, c/no, in the crystal, while the other beam saw an extraordinary refractive index, ne, and travelled with the velocity c/n_e. Since ne and no are normally different in mercurous chloride crystal, two beams propogated at different speeds and arrived at the other end with a different phase relationship. The change in the phase could be detected by recombining the two beams using a polarizer. If the two beams passed through the crystal, the output beam from the polarizer would be uniform in intensity.

To the extent that one or both beams are distorted by the crystal, a fringe pattern similar in appearance to the pattern from a standard interferrometer would be present in the output beam. Details of the schematics are shown in Figure 4.

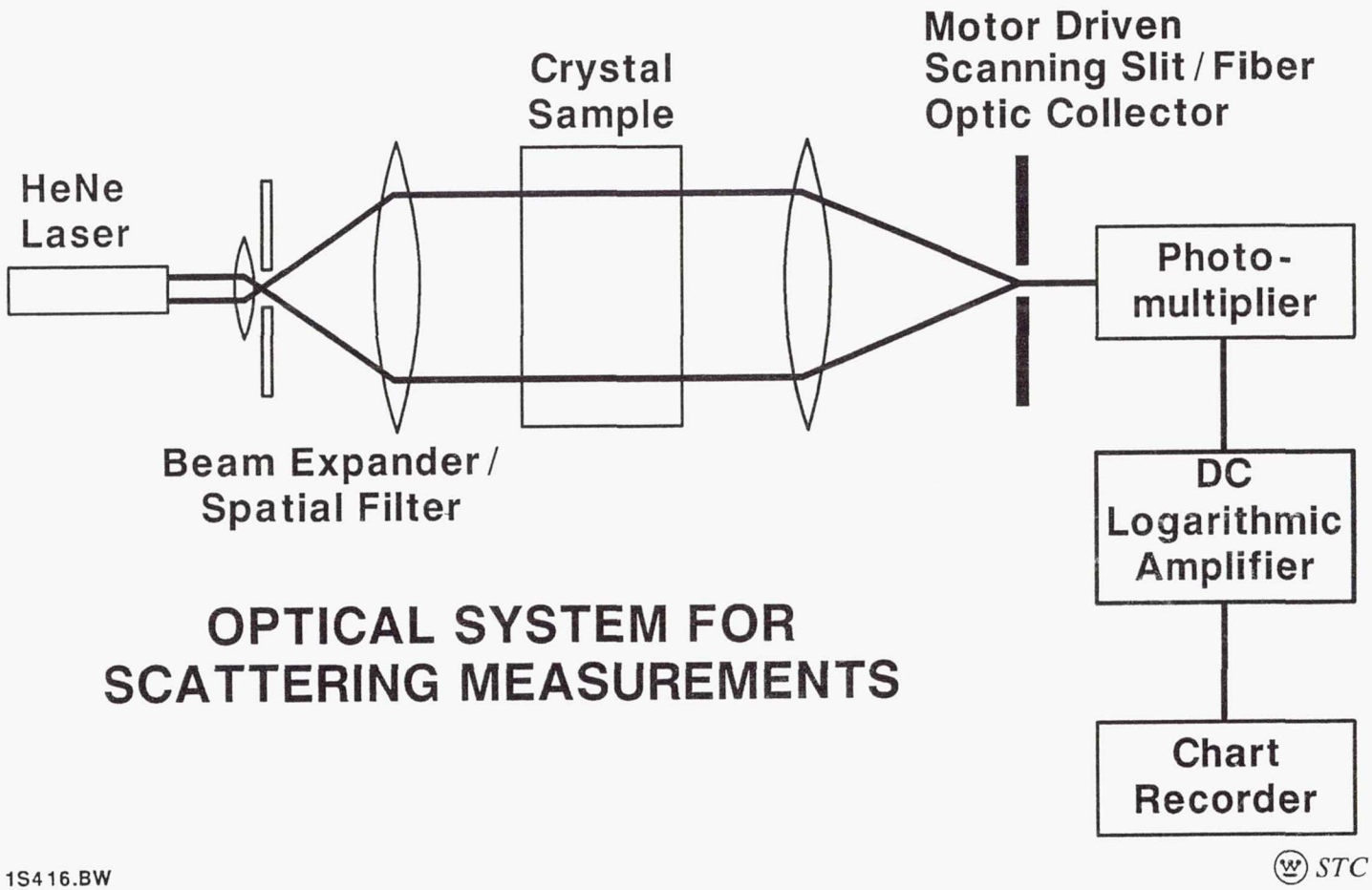

Figure 3. Assembly for scattering measurements.

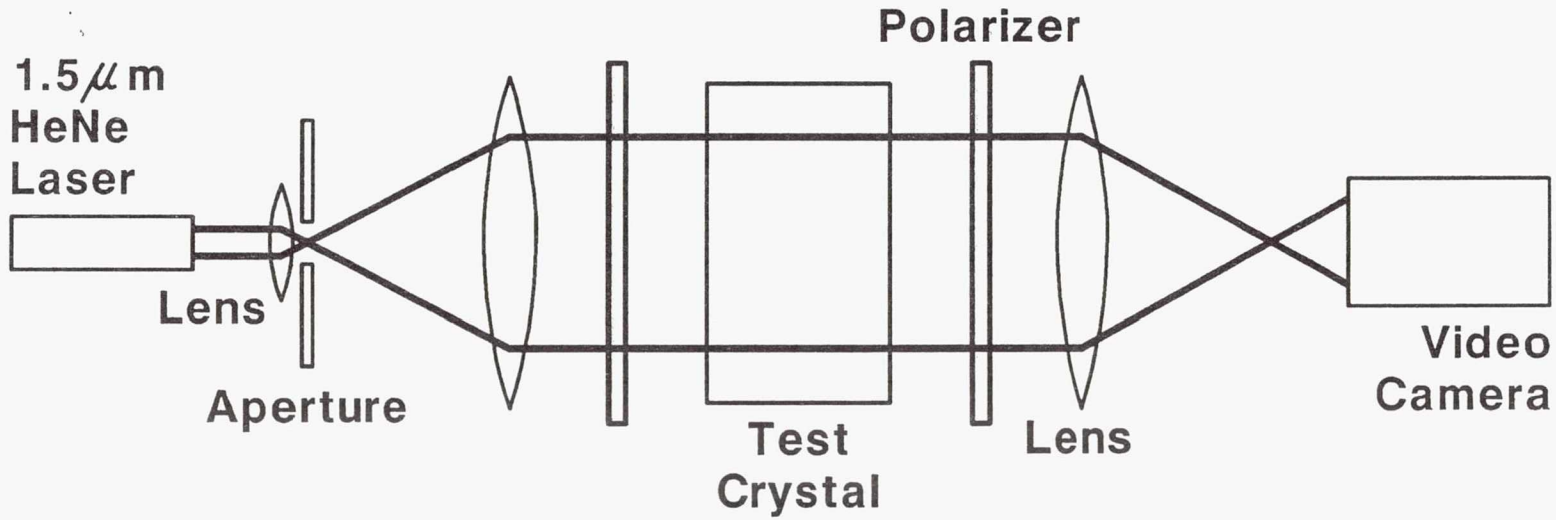

Figure 4. Assembly for birefringence study.

4. RESULTS AND DISCUSSION

4.1 IMPURITIES AND CHARACTERIZATION

During the purification of source material, a large amount of residue was left behind. X-ray analysis was done to match the lines with standard patterns in the Joint Committee on Powder Standards database. The match was to the compound $Hg_5Cl_2O_4$. Diffraction data indicated that this material is orthorhombic, having lattice parameters of a = 11.598 Å, b = 11.717 Å, and c = 6.090 Å. In order to avoid solutal effects and impurity parameter constants, we prepared the material in batches. The purification of mercurous chloride by this method produced source material which contained metallic impurities well below 15 ppm. These results were obtained by spark source mass spectrometry.

4.2 TEMPERATURE DISTRIBUTION

There was very little if any difference in the temperature profile measured by thermocouple and platinum probe. In the case of the platinum probe, the growing crystal and vapor was acting as a medium, while in the case of the bare thermocouple hot air was acting as the medium.

Two sets of observations were made. In the first case the temperature distribution was kept constant and the aspect ratio of the growth tube was changed. The temperature profile is shown in Figure 5. In the second case experiments were carried out to examine the effects of source temperature for the identical aspect ratio.

4.3 GROWTH RATES AND TRANSPORT BEHAVIOR

In the present study experiments were conducted by the PVT process in the region where the Knudsen number was smaller than unity; hence, collisions between vapor molecules dominated. The transport was congruent and constituent molecules of Hg_2Cl_2 transported intact during crystal growth. The present studies and the experiments of Barta et

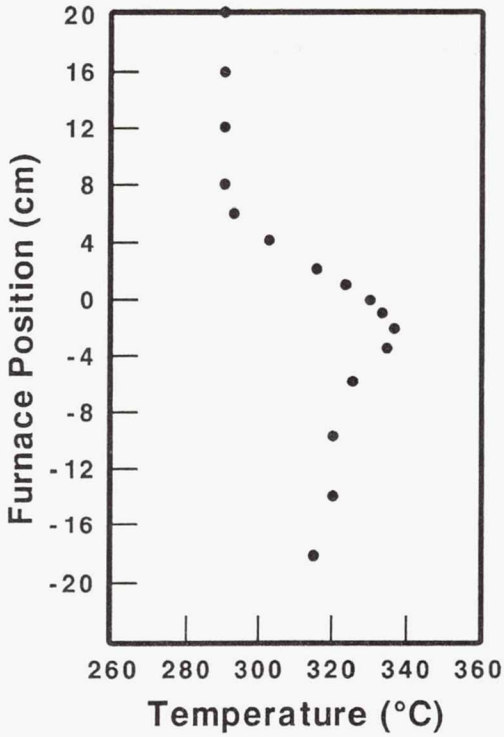

Figure 5. Temperature distribution for growth rate measurements at different aspect ratio.

al.[8] showed that in the presence of moisture, Hg_2Cl_2 oxidizes and tends to decompose into Hg and $HgCl_2$. High-purity mercurous chloride did not decompose and the correct stoichiometry was maintained during transport. Signs of mercury and mercuric chloride were not observed during vapor transport.

Growth rate data for different aspect ratios are shown in Figure 6 in the form of crystal length versus time for the closed tube system. All data were taken in the [110] orientation by using the proper seeding technique and in the region where crystals were well away from the conical seeding section of the growth tube. Measurements close to the seed end were avoided to reduce the capillary effects on relaxation time. The experimental data corresponded to equation 2:

$$L_t = Le - A \exp(-t/T) \qquad (2)$$

where L_t is length at time t, Le is the equilibrium length, T, i.e., $(1/G \cdot \gamma)$, is relaxation time, G is the temperature gradient, γ is the kinetic coeficient, and A is a constant. Similar studies were carried out at a constant aspect ratio and identical thermal conditions for

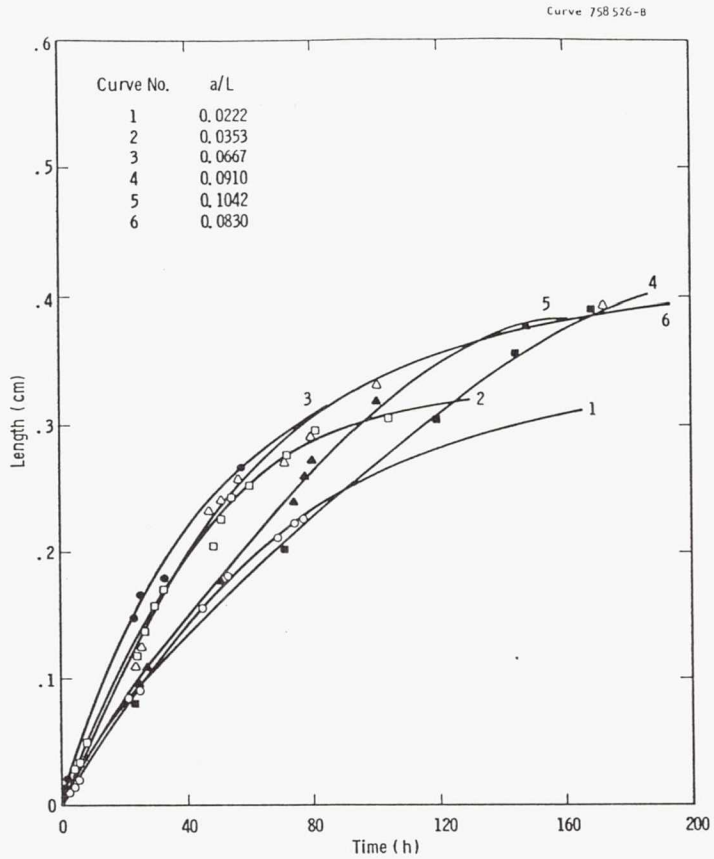

Figure 6. Length of growing crystals as a function of time at different aspect ratio.

crystals where one and two effusion holes were used to permit the elimination or reduction of any impurity. The data are shown in Figure 7. The values of T and γ given in Table 1 showed that the kinetic coefficient was mildly affected by the presence of effusion holes, and relaxation time was similarly affected by the effusion holes. Consequently, there is no definite trend of change, again suggesting that perhaps interfacial attachment kinetics dominate during the growth of Hg_2Cl_2.

The velocity profile across the circular duct is derived by substituting the general expression to the shear stress into Newton's

Table 1
Kinetic Coefficient and Relaxation Time

Growth Condition	γ (cm/K•h)	T (h)	G (K/cm)
Closed Tube	0.011	64	1.4
One Hole	0.013	51	1.5
Two Holes	0.011	65	1.4

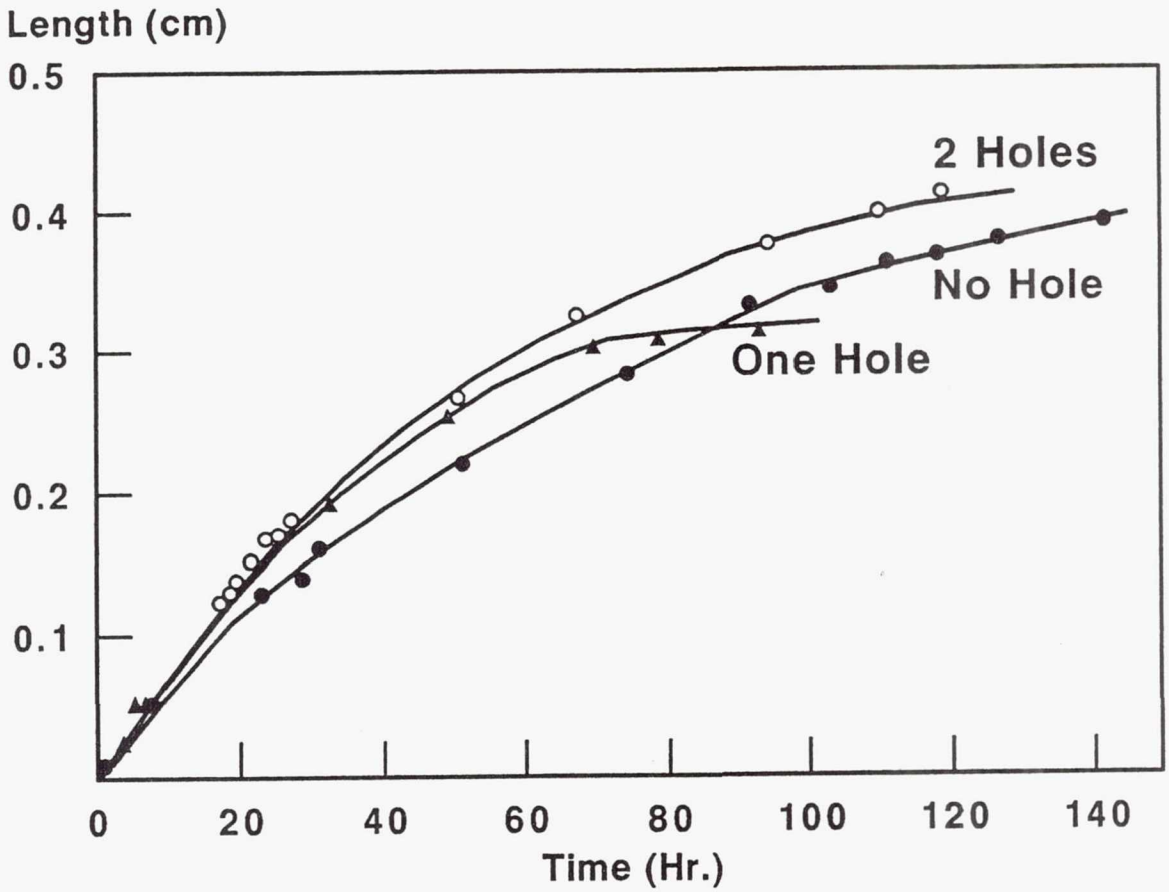

Figure 7. Length of growing crystals as a function of time for no hole, one hole, and two holes at a/L = 0.01.

law of viscosity and integrating by applying the no-slip condition at the wall. The average velocity is defined as:

$$v = \frac{P \cdot a^2}{8 \eta \cdot L} \tag{3}$$

where P = Ps - Pc, Ps and Pc are the vapor pressures at the source and crystal interfaces, η is the viscosity, L the distance between interfaces, and a is the radius of the growth tube. Volumetric flow rate Q can be derived by the following integration:

$$Q = \frac{\Delta P \cdot a^2}{8 \eta \cdot L} \cdot \int_0^a 2 \pi r \, dr \tag{4}$$

hence,

$$Q = \frac{\Delta P \cdot \pi \cdot a^4}{8 \eta \cdot L} \tag{5}$$

a result which is known as the Hagen-Poiseuille equation. In spite of the fact that equation 5 is only applicable to incompressible fluids, one can derive[10,11] the number of moles, N, flowing each second through the cross-section area, which is given as:

$$N = \frac{\pi \cdot a^4}{8 \eta \cdot L \cdot R} (Ps^2 - Pc^2) / (Ts + Tc) \qquad (6)$$

and flux is then:

$$N/\pi a^2 = \frac{a^2}{8 \eta \cdot L \cdot R} (Ps^2 - Pc^2) / (Ts + Tc) \qquad (7)$$

where R is the universal gas constant. Rosenberger et al.[9-11] have derived that growth velocity can be given as:

$$V = \frac{9.6\ a^2 \cdot M\ (Ps^2 - Pc^2)}{\eta \cdot L \cdot \rho \cdot (Ts + Tc)} \qquad (8)$$

where M is the molecular weight and ρ is the density of the solid; T_s and T_c represent the temperatures of source and growth interface as given in Figure 5. When we used the experimental parameters to predict the growth velocity by using equation 8, the experimental growth rate was observed to be orders of magnitude lower than the predicted growth rate. A few researchers have attributed the low transport rates to some other mass transport governed by the impurity redistribution. It is believed that impurities rejected during crystal growth tend to form a boundary layer at the growth interface, and the growth flux tends to accumulate the entrained impurities which are not accepted by the growing interface. This effect has been reduced by allowing the impurities accumulating at the interface to effuse out of the ampoule. In order to test the applicability of this technique to the calomel system, one hole was made in one ampoule and two holes in the other. As shown in Figure 7, no change was observed in the growth rate which could satisfy equation 8. Furthermore, in the case of one effusion hole and two effusion holes, the identical growth velocity was observed. In the case one hole, 37% of the material escaped from the growth tube, and in the case of two holes, 66% of the material was lost. This confirms that differences between observed and predicted growth velocities are not accounted for as the result of an impurity layer boundary forming on the growing interface in the system. In spite of the fact that (Ts - Tc) was small, the Hg_2Cl_2 heated above the temperature of the top end of the

ampoule; in this situation one must expect the influence of convective flow on net flow. For the purpose of estimating the concentration distribution, a one-dimensional diffusion treatment with PVT was used. In an effort similar to that of Rosenberger et al., we selected: (a) the source interface as the reference, (b) steady-state growth conditions, (c) a fixed distance from source to growth interface and ignored the effect of temperature on vapor density between source and growth interface. The molar concentration of Hg_2Cl_2 at distance x from source is given as:

$$C(x) = C - [C - C(0)] \exp (P_e X/L) \tag{9}$$

where C(0) and C are the concentration of Hg_2Cl_2 vapor at the source and total molar concentration. P_e is the Peclet number defined as:

$$P_e = \frac{V L}{D_{AB}} \tag{10}$$

where V is the mole average velocity and D_{AB} is the binary diffusion coefficient. Since we used Hg_2Cl_2, which had less than 15 ppm impurity, equation 10 can be written as:

$$P_e = \frac{V \cdot L}{D_{11}} \tag{11}$$

where D_{11} is self diffusivity. The dependence of concentration on peclet number is shown in Figure 8. The Peclet number predicted by equation 11 is very small (P_e = between 0 and 1) for our system, and a relatively uniform distribution of impurities (if any) is expected. At the large Peclet number (not in this case), the increased Hg_2Cl_2 flux would largely over-ride any back diffusion of impurities. Impurities accumulate at the interface from the diffusion boundary layer, which can limit access to the interface for source material undergoing non-molecular transport.

In addition to density changes in the vapor phase induced by temperature changes, and the associated changes in the vapor pressure over the source and crystallization surfaces, further complexity is created because sometimes both effects compete with one another. The overall motion can be explained in terms of the Rayleigh number. For the geometry used in our system, the Rayleigh number is defined in

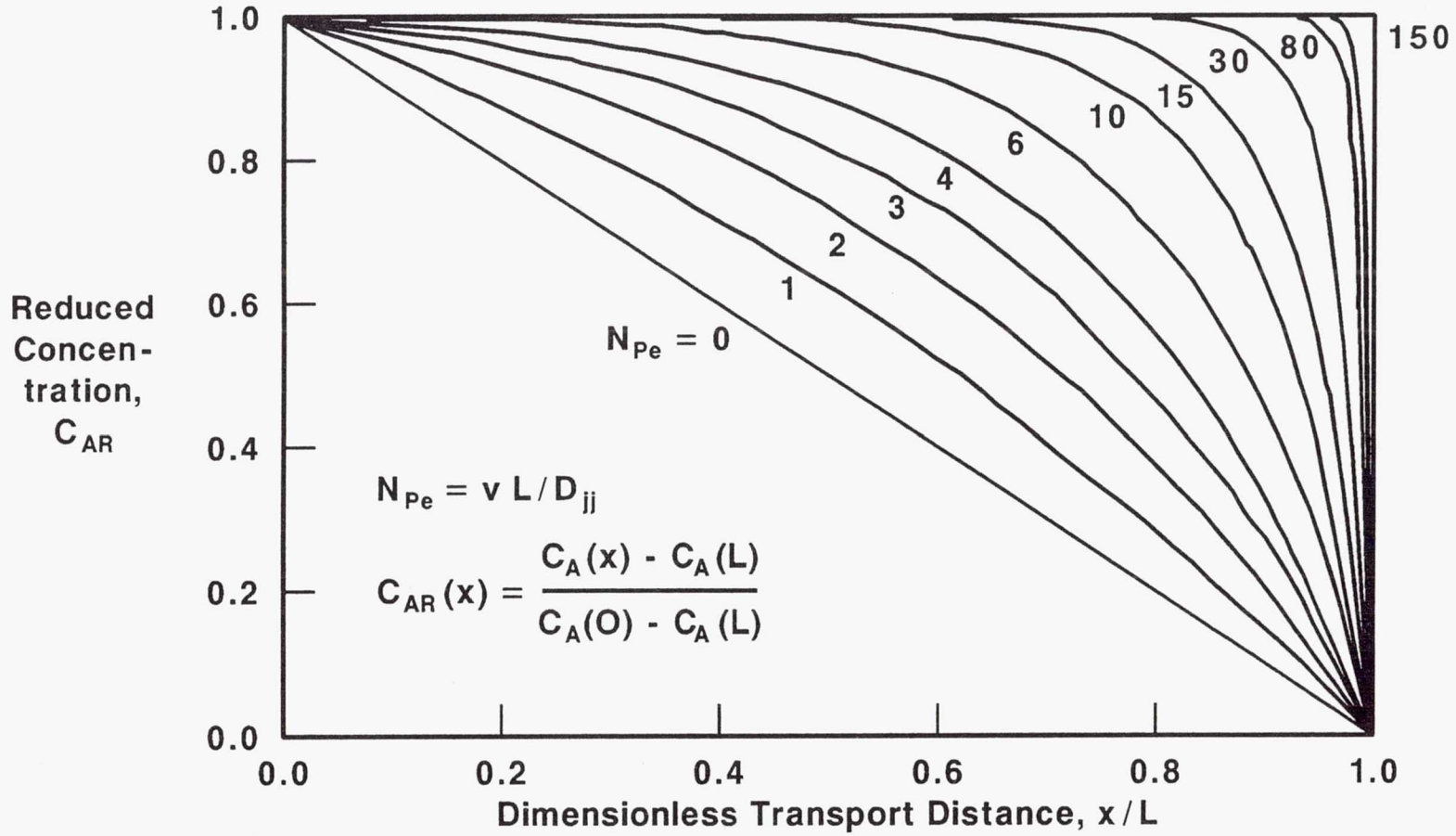

Figure 8. The dependence of concentration on the Peclet number.

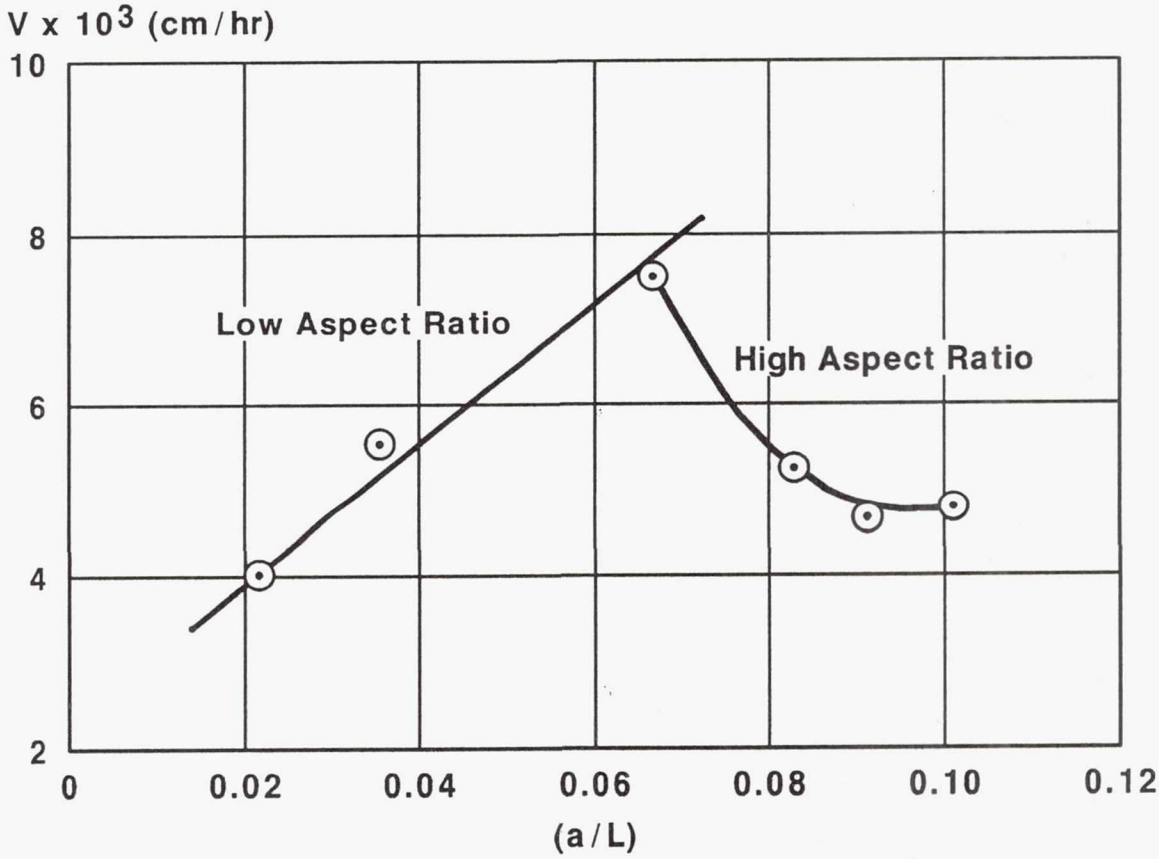

Figure 9. Growth velocity as a function of aspect ratio.

Section 2. Figure 9 shows the experimental growth velocity data for PVT in a cylindrical ampoule for which the aspect ratio varied by an order of magnitude. There was a direct relationship between a^2/L and the flux for both condensing and transporting flux. This occured only up to a certain value of aspect ratio and hence the Rayleigh number. Figure 10 shows the variation of growth velocity in terms of Rayleigh number. It is clear that growth velocity increases with aspect ratio (hence Ra as expected), and then suddenly drops to a value which appears to be constant. This clearly indicates that one cannot scale the system on the basis of measurements in the low aspect ratio region, and in addition suggests that some change in fluid flow behavior is occuring in the growth system. We believe this again confirms that convection increases growth velocity up to certain value; after that, convection destablizes flow in the system. As shown in Figure 10, linear stability theory will not explain the experimental observations.

Since the early 1970s, various fluid dynamists have developed theoretical stability curves for fluid behavior for high aspect ratio

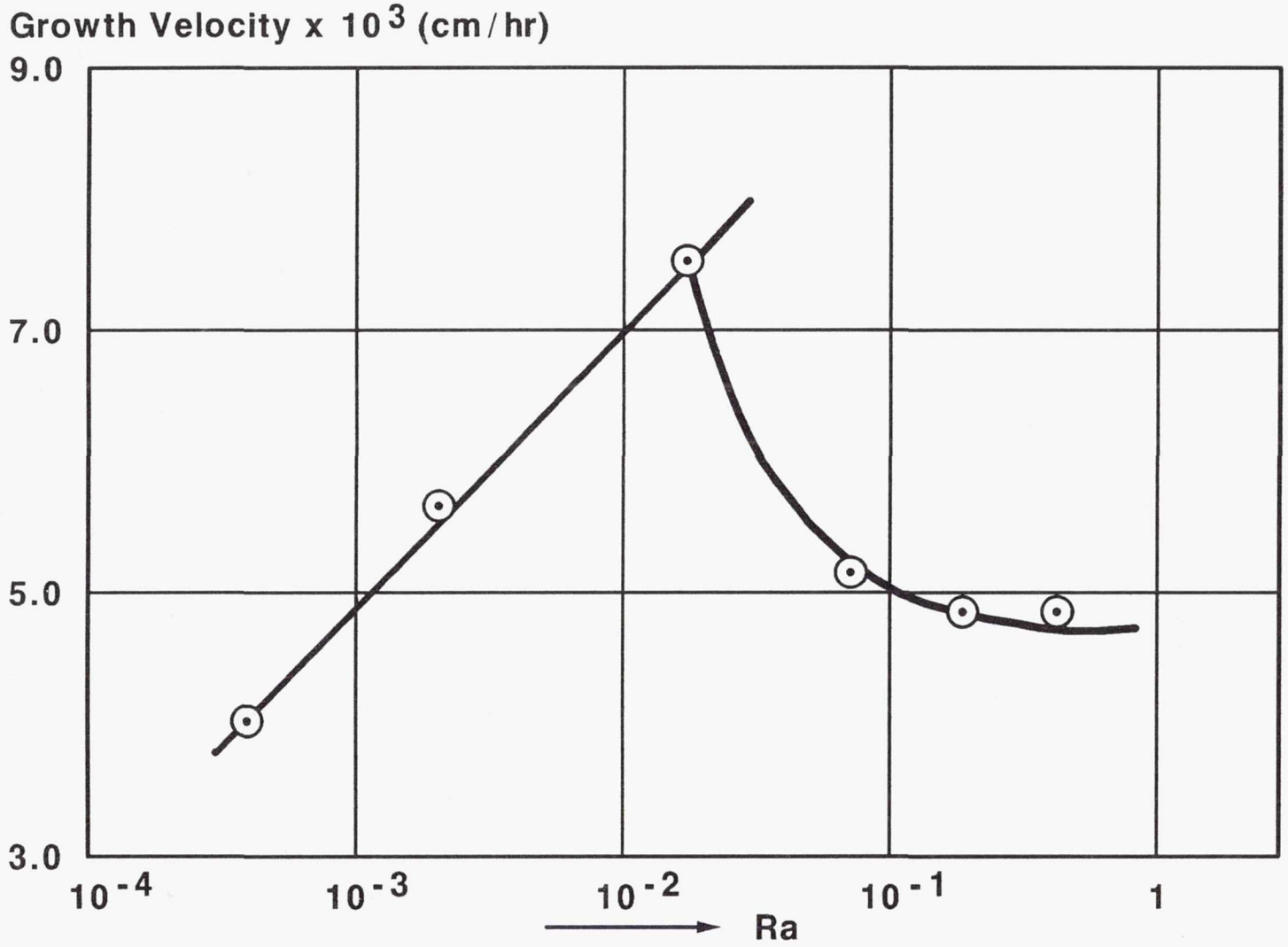

Figure 10. Growth velocity as a function of Rayleigh number.

geometries, especially for fluids having high Prandtl numbers. The case of mercurous chloride is much more complex. The stability curve for Hg_2Cl_2 is shown in Figure 11; for conditions representing the practical crystal growth range and aspect ratio, the stability curve for mercurous chloride is very interesting. It shows a transtion point as the aspect ratio decreases. For the quartz container we observed the transition point at a value of a/L between 0.06 and 0.08. To our knowledge, a theoretical stability curve for an aspect ratio less than 0.1 and for a low Prandtl number fluid has not been developed for this type of geometry.

To study the effect of source temperature on growth rates we carried out experiments where T was varied for one set of experiments at constant a/L. For the physical vapor transport from the high-temperature to the low-temperature zone, the flux can be given as:

$$J = J_H - J_C = (P_H - P_C) \; / \; \sqrt{2 \pi MRT} \qquad (12)$$

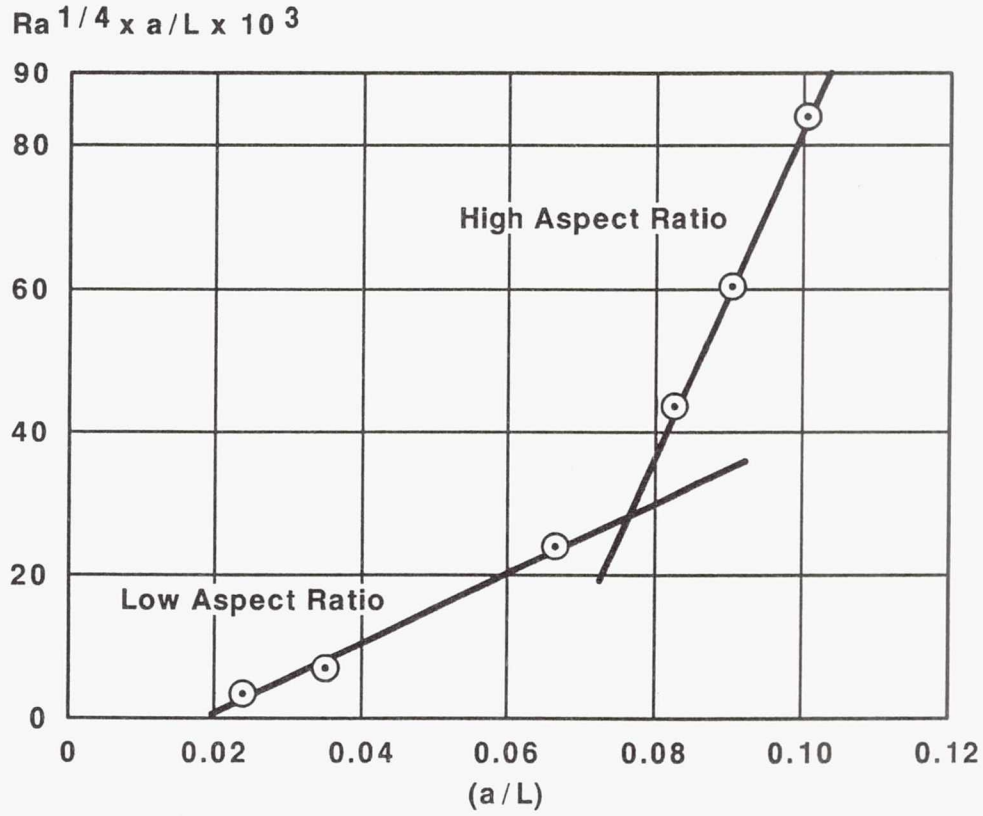

Figure 11. Stability curve for Hg_2Cl_2.

where J_H and J_C are the flux from the hot and cold temperature zone, and PH and PC are the vapor pressure at the hot and cold zone. This equation is applicable for PVT growth in which a certain sink action of the growing surface is assumed. Figure 12 shows the Arrhenius plot of the experimental and theoretical curves. The experimental line corresponds to calculated values corrected by the sticking coefficient of approximate values of 0.01. Since all the growth rate measurements were made in the (110) direction and at the identical aspect ratio, the change in growth rate was attributed to thermal conditions only.

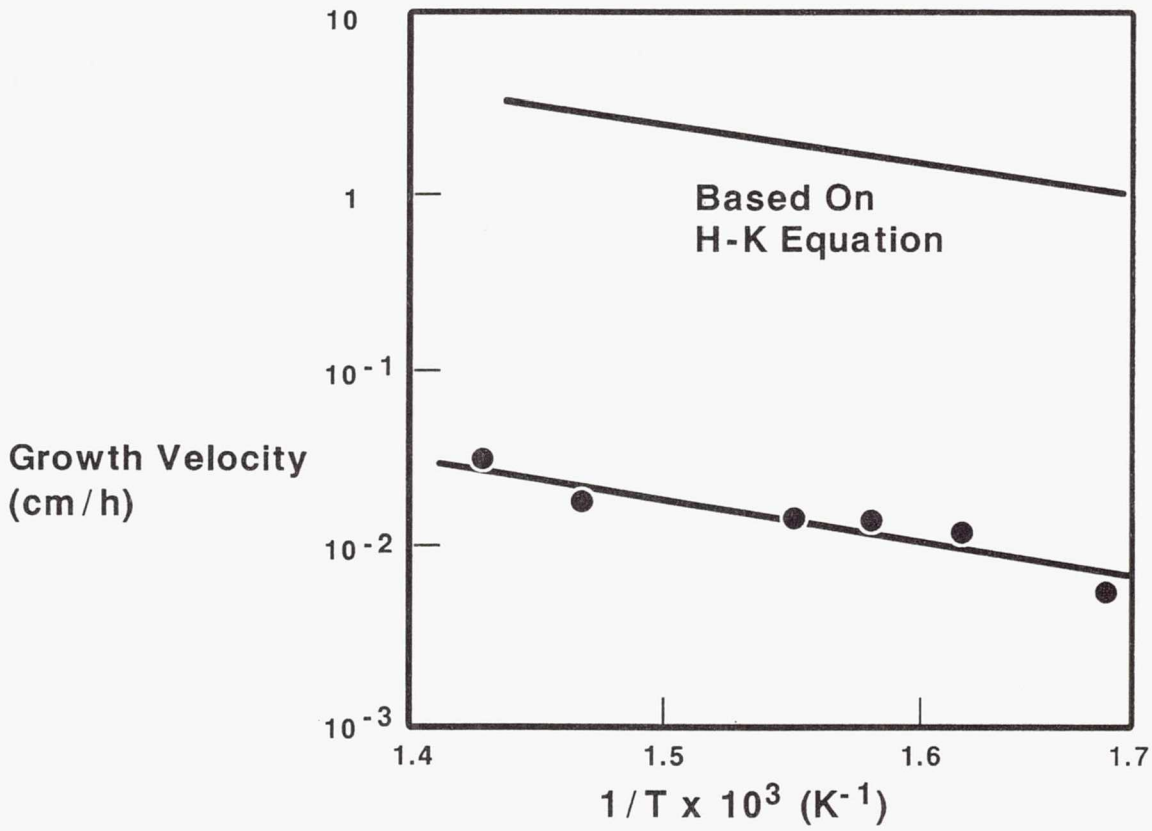

Figure 12. Arrhenius plot for Hg_2Cl_2.

4.4 QUALITY OF CRYSTALS GROWN AT DIFFERENT Ra

The mercurous chloride crystals grown in different thermal conditions were evaluated by measuring the bulk scattering and inhomogeneity of refractive index by birefringence interferometry (Figures 13 and 14). It was clearly observed that crystals grown at higher ΔT showed higher scattering and irregular fringes. Since the

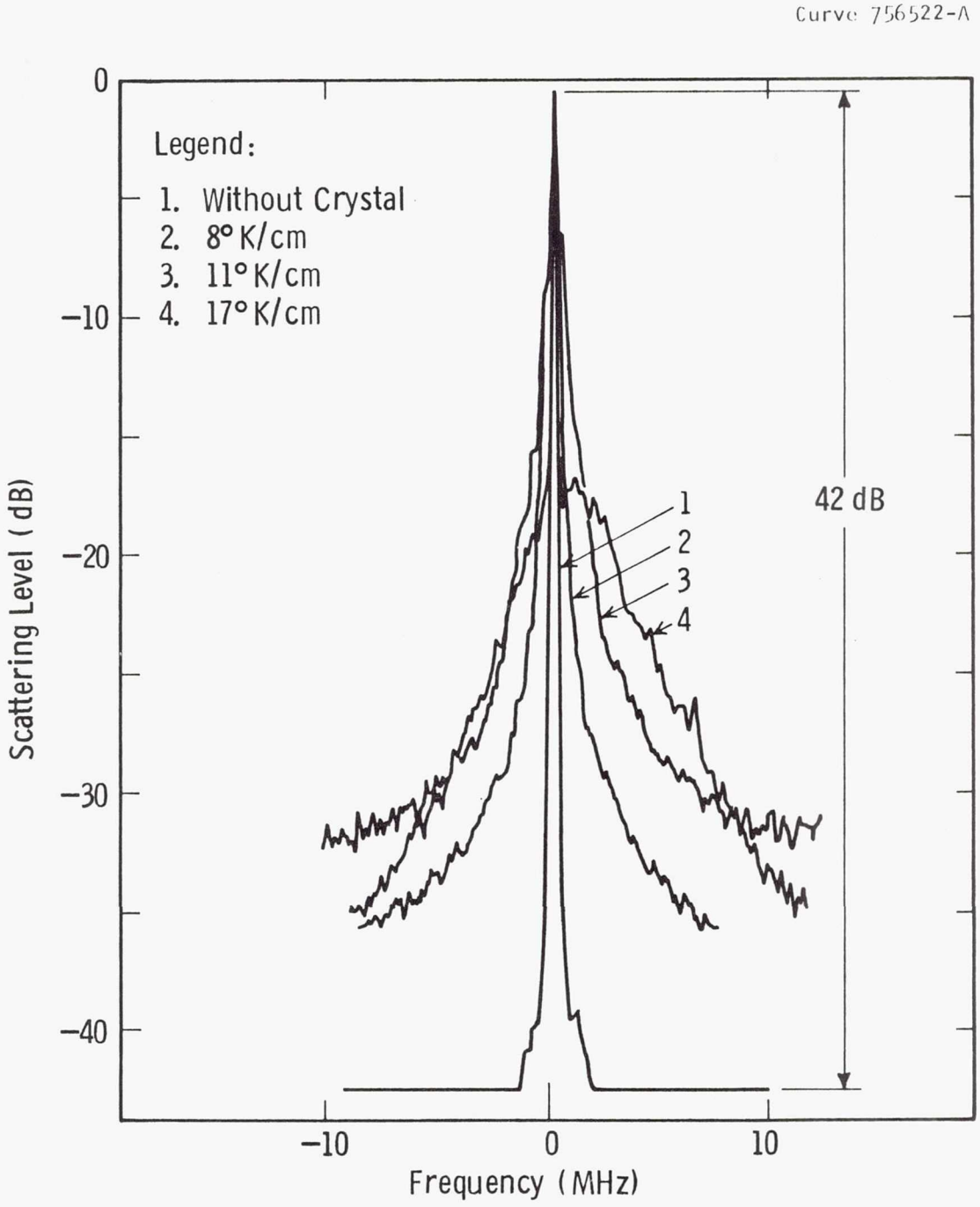

Figure 13. Scattering for crystals grown at different Ra.

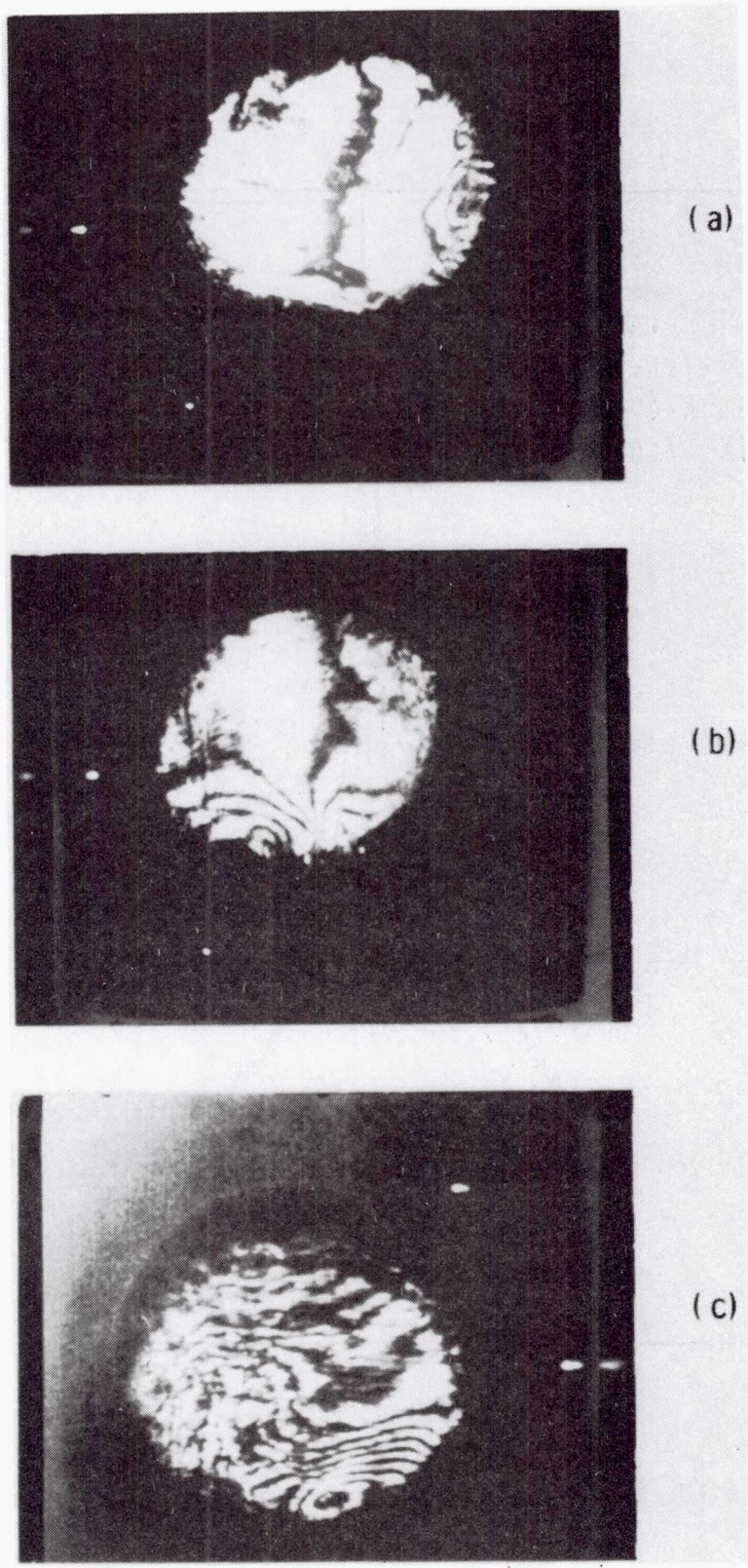

Figure 14. Birefringence interferograms for crystals grown at different Ra: (a), (b), and (c) correspond to 8°K/cm, 11°K/cm, and 17°K/cm, respectively.

crystals were grown from the identical source material and cooling conditions were identical, the difference in homogeneity is attributed to stresses developed in the crystals due to the difference in ΔT and hence Ra.

5. SUMMARY

- The condensing flux at the solid-vapor interface was orders of magnitude lower than the flux calculated by transport theory.
- An increase of 20% in the growth rate was observed in the system with effusion holes in comparison to the closed system. This showed that the difference in growth velocities is not due to impurity boundary layers.
- Theories based on the Hagen-Poiseuille equation could not explain the fluid dynamic phenomena.
- A condensation coefficient is required to explain the growth velocity data of mercurous chloride.
- Growth velocity was observed to be orientation dependent for a low growth rate (low T) region.
- Crystals grown at low Ra showed better quality.

6. PUBLICATIONS FROM PHASE I OF THE PROGRAM

Following are the results of Phase I of the program.

1. "Evaluation of Transport Conditions During PVT Growth: Mercurous Chloride System," Physico Chemical Hydrodynamics 11 (1989), 41.
2. "Effect of Temperature Gradient on the Optical Quality of Mercurous Chloride Crystals," J. Crystal Growth 96 (1989), 916.
3. "On the Quality of Mercurous Chloride Crystals," Materials Letters 7 (1989), 397.
4. "Evaluation of Growth Conditions During PVT of Opto-Electronic Crystals," AIAA Journal of Thermo-Physics and Heat Transfer (Communicated).

For more-detailed information, all of the above-mentioned papers are included as appendices at the end of this report. In addition to the papers cited above, results were presented at the following seminars and conferences.

1. "Growth of Large Crystals of Mercurous Chloride Crystals," Special Symposium on Space Processing, BHU Varanasi, Jan. 13, 1988.
2. "Congruent Vapor Transport in 1-g Conditions," Symposium on Materials Processing in Space, ASM, Materials Science Division, World Materials Congress, Chicago, IL, Sept. 27, 1988.
3. "Physical Vapor Transport Growth of Mercurous Chloride Crystals," CCDS Meeting at Gruman Aerospace Corporation, July 1988.
4. "On the Transport Behavior of Mercurous Chloride," CCDS Meeting, Marshall Space Flight Center, Huntsville, AL, Feb. 13, 1989.
5. "Growth and Characterization of 1-g Grown Mercurous Chloride Crystals," International Symposium on Mercurous Halides, Prague, Nov. 1989.
6. "Evaluation of Growth Conditions of the PVT Process During the 1-g Growth of Mercurous Chloride Crystals," ICCG-8, Sendai, Japan, 1989.

7. FUTURE PLANS

Given the means, objective for future study are:

1. Study the growth rates and kinetics of the PVT process by varying the g-vector.
2. Identify the magnitude of convective effects due to variation of the g-vector.
3. Correlate growth rates with inclination of the g-vector and the quality of grown crystals, keeping the aspect ratio and thermal environments identical.
4. Identify the critical range of convection/diffusion dominating the growth process by studying the growth rate at different thermal environments and different g-vectors.
5. Identify the effects of microgravity with respect to mercurous halide crystal growth and design a microgravity experiment.

A very important outcome of these studies will be to determine the role of microgravity using the PVT process in growing large crystals with improved optical properties in comparision to those grown in 1-g conditions.

8. REFERENCES

1. N. B. Singh, M. Gottlieb and A. Goutzoulis, J. Crystal Growth 82 (1987), 274.
2. N. B. Singh, R. H. Hopkins, R. Mazelsky and M. Gottlieb, J. Crystal Growth 85 (1987), 240.
3. M. Gottlieb, N. B. Singh and A. Goutzoulis, Appl. Opt. 26 (1987), 4681.
4. N. B. Singh, R. H. Hopkins, R. Mazelsky and J. J. Conroy, J. Crystal Growth 75 (1986), 173.
5. I. C. Chang, IEEE Trans. Sonics & Ultrasonics SU-23 (1976), 7.
6. N. B. Singh, R. H. Hopkins, R. Mazelsky and M. Gottlieb, J. Crystal Growth 85 (1987), 240.
7. S. J. Yosim and S. W. Mayer, Am. Chem. Soc. 64 (1960), 909.
8. C. Barta, Krist. und Tech. 5 (1970), 541.
9. F. Rosenberger, Physico-Chemical Hydrodynamics 1 (1980), 3.
10. J. R. Carruthers, Preparation and Properties of Solid State Materials, Ed. by Wilcox (Marcel Dekker Inc., New York, NY), Vol. 4 (1979), 50.
11. J. R. Abernathey, D. W. Greenwell and F. Rosenberger, J. Crystal Growth 47 (1979), 145.
12. G. S. Charlson and R. L. Sani, J. Heat Mass Trans. 14 (1971), 2157.

ACKNOWLEDGMENTS

The author is grateful to NASA, Microgravity Science and Application Division, Code EN, for providing the financial assistance of Contract NAS3-25274 through NASA Lewis Research Center.

NASA
National Aeronautics and Space Administration

Report Documentation Page

1. Report No.	2. Government Accession No.	3. Recipient's Catalog No.
NASA TM - 103788		

4. Title and Subtitle	5. Report Date
Growth Kinetics of Physical Vapor Transport Processes: Crystal Growth of the Optoelectronic Material Mercurous Chloride	March 1991
	6. Performing Organization Code

7. Author(s)	8. Performing Organization Report No.
N.B. Singh and W.M.B. Duval	E - 6065
	10. Work Unit No. 674 - 21 - 05

9. Performing Organization Name and Address	11. Contract or Grant No.
National Aeronautics and Space Administration Lewis Research Center Cleveland, Ohio 44135 - 3191	
	13. Type of Report and Period Covered Technical Memorandum
12. Sponsoring Agency Name and Address National Aeronautics and Space Administration Washington, D.C. 20546 - 0001	14. Sponsoring Agency Code

15. Supplementary Notes

N.B. Singh, Westinghouse Science and Technology Center, 1310 Beulah Road, Pittsburgh, Pennsylvania 15235 (work funded under NASA Contract NAS3 - 25274). W.M.B. Duval, NASA Lewis Research Center. Responsible person, W.M.B. Duval, (216) 433 - 5023.

16. Abstract

The results reported here were carried out in order to derive a quantitative understanding of the physical vapor transport (PVT) process for the purpose of identifying the magnitude of convective effects on the crystal growth process. The effects of convection on crystal quality were studied by varying the aspect ratio and those thermal conditions which ultimately affect thermal convection during PVT. An important outcome of the present study was the observation that the convection growth rate increased up to a certain value and then dropped to a constant value for high aspect ratios. This indicated that a very complex transport had occurred which could not be explained by linear stability theory. Better quality crystals grown at a low Rayleigh number confirmed that improved properties are possible in convectionless environments.

17. Key Words (Suggested by Author(s))	18. Distribution Statement
Physcial vapor transport Crystal growth Mercurous chloride Optoelectronic material	Unclassified - Unlimited Subject Category 29

19. Security Classif. (of the report)	20. Security Classif. (of this page)	21. No. of pages	22. Price*
Unclassified	Unclassified	30	A03

NASA FORM 1626 OCT 86

*For sale by the National Technical Information Service, Springfield, Virginia 22161